Chapter 6

Investigation of Mu Yield

The determination of the muonium yield was made by a comparison between the Monte Carlo simulation and the data in a region of the vacuum chamber relatively far from the target. Figure 6.1 shows a density plot of the number of muon decays, in space, as calculated by the extrapolation of decay positron trajectories. The definitions of these regions in space were given in table 4.1. In order to minimize the effect of background from target muon decays, region 2 was selected for comparison to the Monte Carlo. This region had a signal to noise ratio of between 1 and 0.35 depending on changes made to the experimental apparatus for the MUBAR experiment.

For each of the regions R1, R2, R3, and Target, the time of decay of the muons was plotted. Figure 6.2 shows these time spectra for each of the four regions. The muonium signal can be seen as a nonexponential time dependence introduced by the motion of muonium into and out of the different regions.

An average velocity can be calculated by dividing the distance of the muon from the target by the time of decay. An additional correction due to the time acceptance of the apparatus was incorporated into the Monte Carlo through the modeling of the experimental geometry. Figure 6.3 shows a plot of a typical velocity spectrum along with a histogram of the spectrum which is predicted by the Monte Carlo. The agreement is good indicating thermal emission. In addition, no change in yield is noted when an electric field of

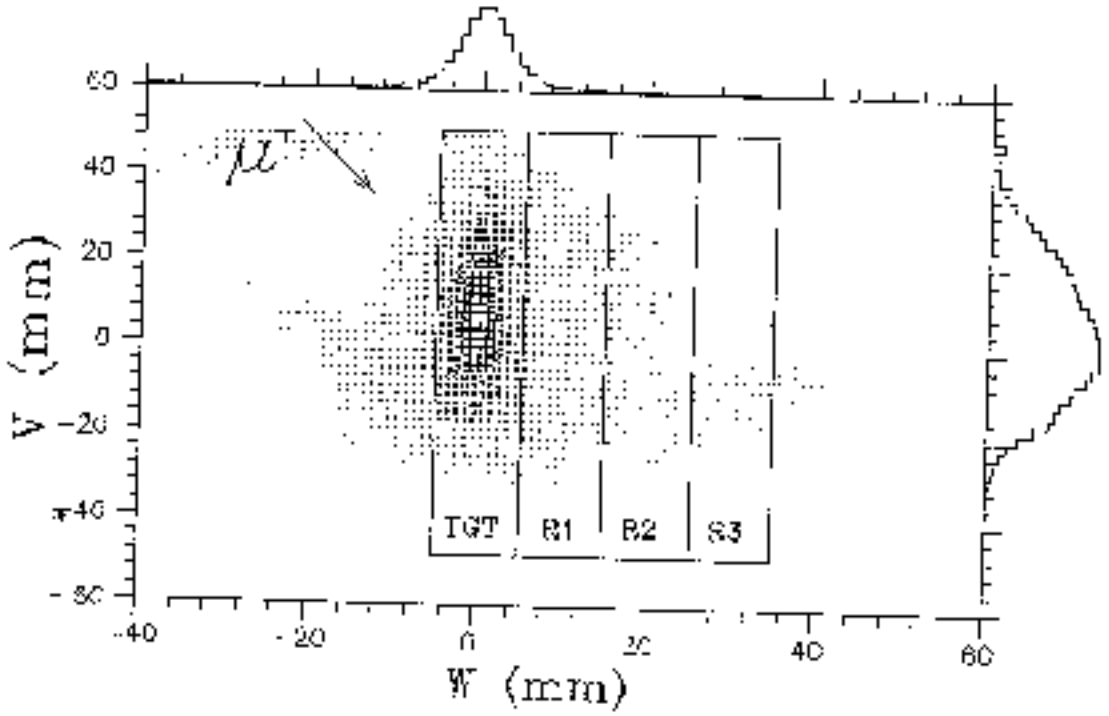

Figure 6.1: Density plot of position of muon decays in space. Yield was determined on the basis of analysis of region 2.

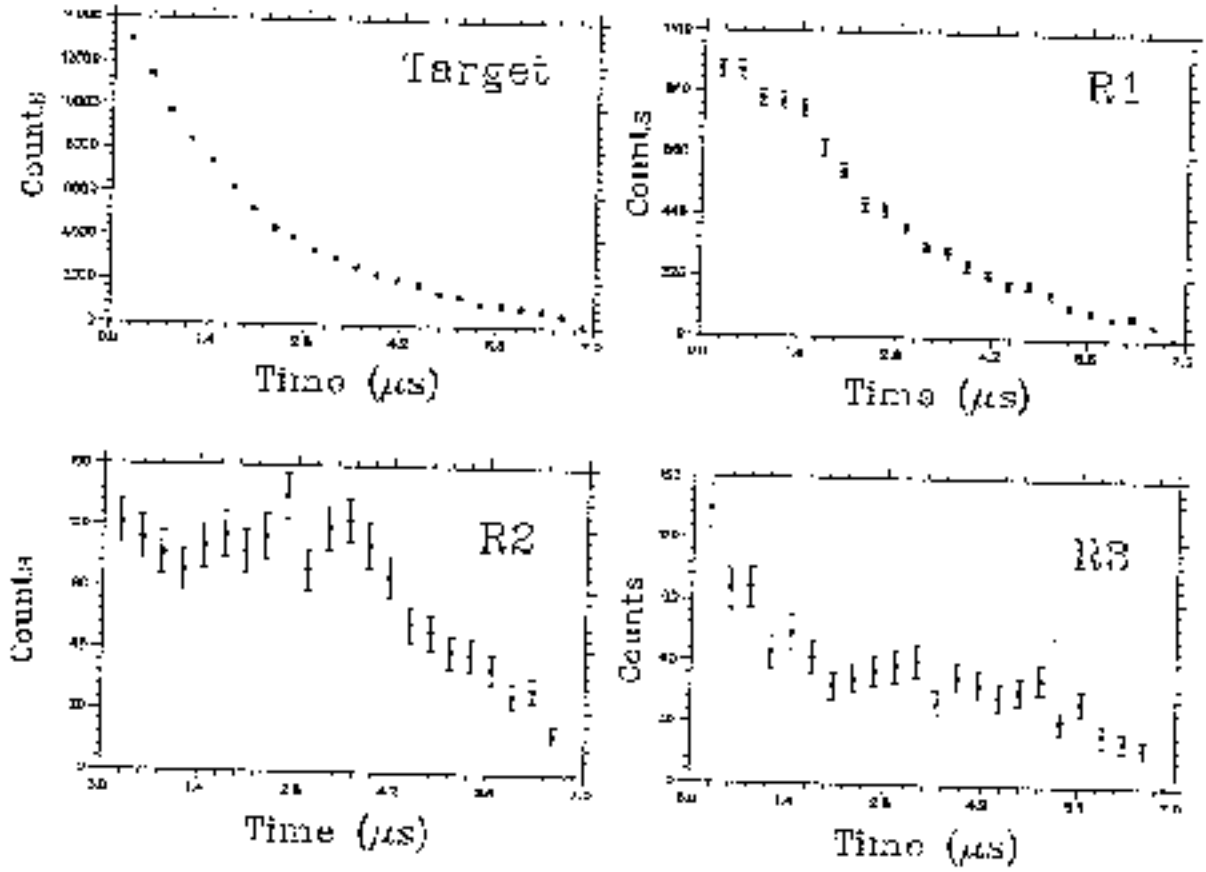

Figure 6.2: Muon decay times for various spatial regions.

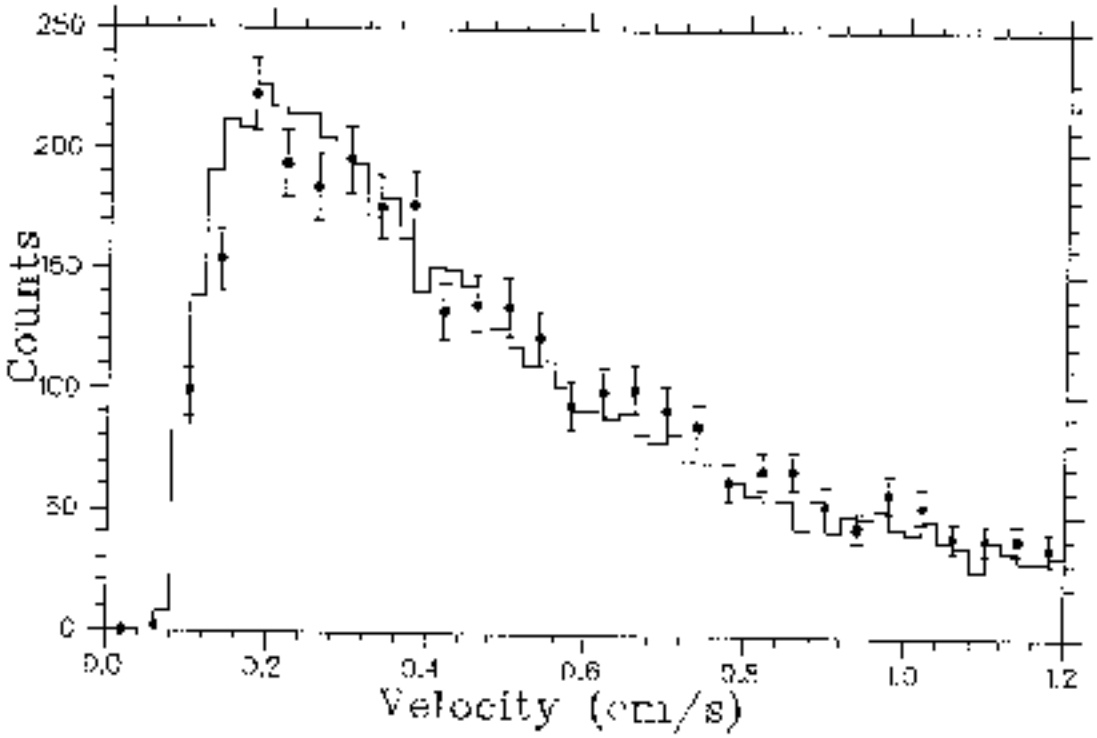

Figure 6.3: Velocity spectrum of muonium with histogram of the spectrum predicted by the Monte Carlo.

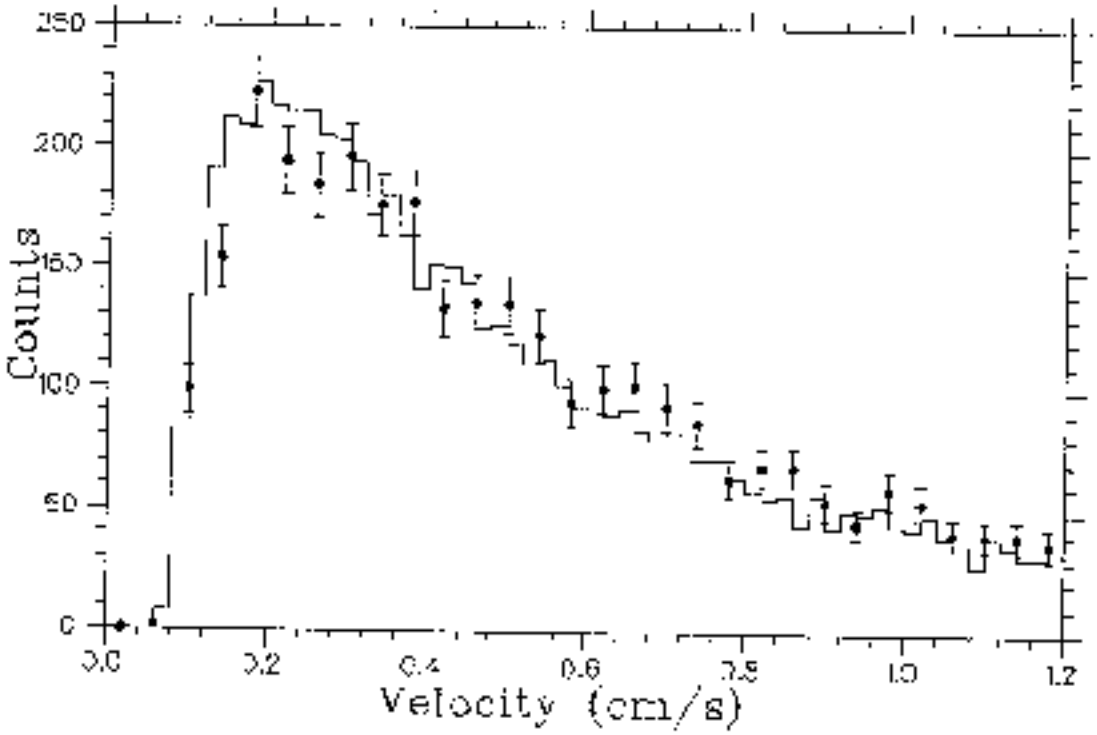

Figure 6.3: Velocity spectrum of muonium with histogram of the spectrum predicted by the Monte Carlo

centre of the cube in place of the target, and the spot size of the beam was minimized. Ranging was done by inserting the catcher next to the target and, with beam momentum, adjusting the relative numbers of stops in both. In 1987, in order to perform other tests related to the MUBAR experiment, tuning and ranging were without the cube in place. The beam focus was only approximately located in the centre of the cube, and ranging was done by inserting material into the beam and measuring the range width of the beam. As a result of tuning, the beam spot on the target was approximately 9% larger in 1987. With the 1987 method of ranging the catcher data, which was necessary to estimate the width of the stopping distribution in the target, was not taken. This width depends on target inhomogeneities and since the physical targets and methods of powder layer preparation were identical, the target inhomogeneity for the 1987 data was taken to be the same as that for 1988.

The targets themselves consisted of an Al support ramp of dimensions 5 mm × 13 mm × 0.010 mm, suspended at an angle of 66° to vertical. The average powder layer thickness was 8.8 mg/cm^2. In order to produce the maximum amount of muonium the target was made as large as possible. As a result a portion of the target, $\sim \frac{1}{3}$ of the length, was out of the field of view of the wire chambers. This experimental geometry was incorporated into MUBEAM which corrected for the fact that a portion of the important vacuum region r2 was out of the field of view. In order to check this correction, a target was constructed which was similar except that the size was only 4.5 mm × 8 mm and it was suspended at 60°. With this target the entire region R2 was visible with the wire chambers. The yields of the 60° target, which will be discussed further below, were consistent with those of the 66° target indicating that the geometrical correction was not a source of systematic error.

For both the 1987 and 1988 MUBAR targets the beam momentum was

Run	Date	SiO_2 mg/cm^2	$\frac{\Delta p}{p}$ %	Yield / tgt stop %	Yield / inc. μ^+ %
115	1987	8.5	10	4.2 ± 1.0	2.4 ± 0.6
116	1987	8.5	10	2.6 ± 0.7	1.5 ± 0.4
117	1987	8.5	10	3.8 ± 1.0	2.2 ± 0.6
118	1987	8.5	10	3.8 ± 0.9	2.2 ± 0.5
Weighted mean			10	3.4 ± 0.4	2.0 ± 0.2
119	1987	8.5	3	4.3 ± 1.1	2.2 ± 0.6
120	1987	8.5	3	4.4 ± 1.2	2.3 ± 0.6
Weighted mean			3	4.3 ± 0.8	2.2 ± 0.4
314	1988	9.1	3	5.3 ± 1.3	2.5 ± 0.6
315	1988	9.1	3	2.3 ± 0.9	1.1 ± 0.4
Weighted mean			3	3.3 ± 0.7	1.5 ± 0.6
345	1988	9.1	10	4.8 ± 1.1	2.6 ± 0.6
362	1988	8.7	10	4.5 ± 1.1	2.5 ± 0.6
369	1988	8.7	10	2.3 ± 0.6	1.2 ± 0.3
370	1988	8.7	10	2.6 ± 0.7	1.4 ± 0.4
Weighted mean			10	2.7 ± 0.5	1.4 ± 0.3
387	1988	8.3	10	3.8 ± 0.9	2.1 ± 0.5
406	1988	8.4	3	5.2 ± 1.2	2.5 ± 0.6
441	1988	8.4	3	6.3 ± 1.0	3.0 ± 0.5
Weighted mean			3	4.7 ± 0.8	2.2 ± 0.4
407	1988	8.4	10	4.5 ± 2.1	2.4 ± 0.6
442	1988	8.4	10	5.9 ± 1.6	3.2 ± 0.9
443	1988	8.4	10	5.2 ± 1.3	2.8 ± 0.7
Weighted mean			10	4.9 ± 0.9	2.6 ± 0.5

Table 6.1: Yields calculated for targets used in the MUBAR experiment in both 1987 and 1988 runs. The weighted means were calculated using the total uncertainty including both statistical and systematic contributions.

Run	SiO_2 mg/cm^2	P MeV/c	$\frac{\Delta P}{P}$ %	Fr. in Target	Yield / tgt stop %	Yield / inc. μ^+ %
72	13	24.3	10	0.56	7.5 ± 1.9	4.1 ± 1.0
79	13	24.3	3	0.56	7.9 ± 1.9	4.4 ± 1.1
80	13	23.8	3	0.67	6.2 ± 1.7	4.2 ± 1.2
87	13	23.2	3	0.80	2.9 ± 0.8	2.3 ± 0.7
82	13	22.6	3	0.90	1.5 ± 0.5	1.3 ± 0.5
86	13	21.8	3	0.96	0.5 ± 0.5	0.4 ± 0.4
455	17.9	28.2	10	0.51	4.5 ± 1.0	2.4 ± 0.6
456	17.9	28.2	3	0.51	7.4 ± 1.7	3.7 ± 0.8
460	17.9	27.9	3	0.61	6.5 ± 1.5	4.0 ± 0.9
461	17.9	27.6	3	0.71	5.1 ± 1.2	3.6 ± 0.8

Table 6.2: Yields obtained with beam momentum scans on two targets to probe the yield as a function of stopping depth in the powder. Included is the fraction of incident muons which stop in the target at specific momenta as calculated by the Monte Carlo.

to the surface of the powder as possible so as not to have too much material through which the muons must diffuse. To examine this effect more closely, yield data was taken at several different beam momenta, effectively probing the muonium yield as a function of the stopping depth in the powder. The data was taken in a MUBAR run of 1988 and in a development run in 1986.

The target of the 1988 data is the 60° target described above with a thick Cab-O-Sil layer of 18 mg/cm^2. The 1986 target was of dimension 4.5 cm × 7.5 cm, also suspended at an angle of 60° to the vertical, and had a powder thickness of 13 mg/cm^2. While both data sets in the momentum scan were taken with a narrow (3%) momentum bite, the 1988 beam momentum was ∼ 28 MeV/c and the 1986 momentum was ∼ 24 MeV/c. Table 6.2 lists the data which was taken in 1986 and 1988 including the momenta, momentum bite, and the fraction of incident muons which stopped in the target. For each target one run was taken at wide momentum bite for comparison with the MUBAR targets. Also listed are the muonium yields both per incident muon

and per muon stopped in SiO_2. In figure 6.6 both of these yields, determined from the narrow momentum bite data of varying momenta, are plotted as a function of the fraction of the beam which stopped in the target. From these plots it can be seen that while the yield per SiO_2 stop steadily decreases as the beam is stopped further back into the powder, the total Mu yield reaches a maximum not at a 50% fraction but rather at approximately 60% of the beam stopped. The reason for this is the combination of two competing effects which are responsible for the total yield. Firstly, in order for a Mu to be produced, a muon must stop in the Cab-O Sil. It follows that more stops in the SiO_2 will increase the amount of muonium produced in the target. However, the muonium must also diffuse out of the powder, and the probability of getting out decreases with the depth into the layer at which the Mu atom is formed. Therefore in order to produce the maximum yield of Mu per incident muon, the beam should be ranged so that 60% of the muons stop in the target and the rest pass straight through.

Another target which was studied was a very thin target with 2.8 mg/cm^2 of Cab-O-Sil. The yield per target stop for this target was $(15.0 \pm 3.6)\%$ for a narrow momentum bite and $(15.6 \pm 3.6)\%$ for a wide momentum bite. The yields per incident muon were $(7.6 \pm 1.7)\%$ for narrow and $(5.8 \pm 1.4)\%$ for wide momentum bite. These are consistent with results measured previously with a similar target [23]. That these yields are higher than the yields from the thicker targets could again be due to the relative size of the powder inhomogeneities. Say, for example, that making a powder target introduces a variation in the thickness of the layer of $\sim$20 %. In absolute terms this corresponds to a smaller number of grams per square centimeter for a thin target than for a thick target. So the stopping distribution in a thick target will contain a greater amount of widening which results in more muons stopping further from the surface of the layer.

In order to measure the backgrounds in this experiment nitrogen was introduced into the vacuum chamber. The dependence of the Mu yield on gas pressure has been studied in connection with this background estimation. Using the thin targets of 2.8 mg/cm^2, different pressures of nitrogen were introduced into the chamber and the yields were measured at each pressure. Figure 6.7 shows the Mu yield per SiO_2 stop as a function of N_2 pressure. At a pressure of $\sim$ 1 Torr the thermal Mu signal is completely quenched. This quenching of yield with N_2 is also a measure of the cross section of the collision of Mu atoms with N_2 molecules. Using the yield from vacuum region 2 and MUBEAM, the mean free path of the Mu atoms was calculated for each pressure of N_2. Then equation (6.17) can be used to obtain a value for the distance of closest approach, d. Using the Bohr radius of a Mu and the radius of a N_2 molecule, a geometric estimation of 2×10^{-8} cm was calculated. Quenching the yield with 6 mTorr of N_2 implied a value for d of $(1.9 \pm 1.0) \times 10^{-8}$ cm, and using 20 mTorr of N_2 implies a distance of $(2.5 \pm 1.2) \times 10^{-8}$ cm. Both of these are consistent with the above approximation.

Yield measurements with other physical forms of SiO_2 were performed in order to better understand what properties of Cab-O Sil allow it to produce such a large amount of muonium. No yield was observed from a Cab O-Sil target which had been compressed [23], indicating that the microscopic structure of a material, and not just its chemical composition, is an important property in determining whether a material will produce muonium in vacuum.

Another form of SiO_2 which was investigated was Opti-Pur made by Merck. This is an extremely pure crystaline powder of SiO_2 developed for use in the manufacture of optical fibers. While it is dense compared with Cab-O-Sil, having a density of 0.5? g/cm^3, it has a surface area of 600 m^2/g which exceeds that of Cab-O-Sil. The total yields from this powder are (1.9 ± 3.5) % for a wide momentum bite and (2.8 ± 0.4) % for a narrow momentum bite. Both

measurements were taken at a beam momentum of 28.5 MeV/c. These yields are comparable to those from Cab-O-Sil.

A form of low density SiO_2 is aerogel. This is a silica gel which has been dried under high gas pressures so it keeps its form instead of collapsing in on itself. It has a density of 0.136 g/cm^3, and a high surface area of typically 500-800 m^2/g depending on the density [29,30]. The form of aerogel is a solid transparent block which was cut to a convenient size with a sharp knife. The aerogel target was tried but it proved to be a poor producer of Mu, giving a yield per incident muon of only (0.7 ± 0.2) % with narrow momentum bite. An attempt was made at cleaning the surface of the aerogel by bleeding $\sim$ 20 mTorr of O_2 into the vacuum chamber and sparking a plasma. The yields after this procedure were further reduced by approximately 50 %.

By considering the aerogel and Merck targets it is apparent that a measurement of a single quality of a material, such as density or surface area, is not sufficient to predict the muonium production capability of that material. While like Cab O-Sil, aerogel is also composed of chains of silica particles of small diameters, those chains are crosslinked to produce a sort of skeletal support for its solid form. In Cab-O-Sil the chains are entwined but not firmly connected. Another characteristic which is important for aerogel is pore size. The type of aerogel used would have a maximum pore size of $\sim$20 nm. However, exposure to moisture preferentially decreases size of the largest pores [30] by as much as a factor of 4 in some cases. The macroscopic structure is not changed nor is the measured surface area. This could perhaps explain the reduction in yield following plasma cleaning.

Recently Woodle et al. [31] at SIN have also measured the yield of thermal muonium from Cab O-Sil. An incident beam of 20.1 MeV/c and width 1.5 Mev/c was used. The target thickness was 0.0 mg/cm^2. The yields obtained for EH5 were (18 ± 2)% of the stopped muons and (11 ± 2)% of the in

coming muons. The diffusion constant was calculated to be (1068 ± 81) cm^2/s. The apparatus used was quite similar but no data which is directly comparable was collected by the MUBAR group. To make a comparison, a Monte Carlo simulation was run using the diffusion constant inferred from this work, 620 ± 80 cm^2/s, in the configuration of the SIN experiment. When the target was assumed to be perfectly homogeneous the simulated yields calculated were (8.2 ± 0.4)% of the incident muons, or (17 ± 1)% of the stops in the Cab-O-Sil. If, however, the targets were assumed to have an inhomogeneity of 30% of the target thickness, comparable to the targets used in this work, then the simulated yields were (4.9 ± 0.3)% of the incident muons, or (9.9 ± 0.6)% of the stops in the Cab-O-Sil. The errors quoted represent the uncertainty in the above diffusion constant. The variation in the simulated yields gives an indication of the importance of considering the target inhomogeneity in the modeling of the stopping distribution in the target.